Renewable Energy 76 (2015) 303–311

Contents lists available at ScienceDirect

Renewable Energy

journal homepage: www.elsevier.com/locate/renene

Effects of vortex generators on a blunt trailing-edge airfoil for wind turbines

Linyue Gao*, Hui Zhang, Yongqian Liu, Shuang Han

State Key Laboratory of Alternate Electrical Power System with Renewable Energy Sources, North China Electric Power University, Beijing 102206, China

ARTICLE INFO

Article history:
Received 10 April 2014
Accepted 16 November 2014
Available online 2 December 2014

Keywords:
Vortex generator
Blunt trailing-edge airfoil
Flow separation
Numerical simulation
Wind turbine

ABSTRACT

Vortex generators (VGs) are commonly-used effective flow separation control devices, and are proved to have potential to improve the aerodynamic performance of large wind turbines. In this paper, the flow physics of VGs and how their size affects the aerodynamic performance of a blunt trailing-edge airfoil DU97-W-300 have been investigated using CFD simulations. Based on wind turbine dedicated airfoil with and without VGs respectively, three-dimensional numerical models were established and further validated through the comparisons between the numerical results and the experimental data. The effects of VGs' size were analyzed from several perspectives, such as trailing-edge height, length, short and long spacing between an adjacent pair of VGs. The results indicate that drag penalty is more sensitive to the increase of VG height than lift; an increment of VG length leads to negative effects on both lift and drag; increases of the spacing between an adjacent pair of VGs have positive impact on suppression of separated flow. Additionally, the flow field characteristics were further revealed by the analysis of streamlines and vortices in the wake region.

1. Introduction

In order to achieve strong structure for large wind turbine blades, thick airfoils have been designed and researched to absorb large bending loads, which are applied from middle to the root sections of blades in recent years [1,2]. Compared with normal thick airfoils, blunt trailing-edge airfoils are dedicated wind turbine airfoils, which are able to be adopted in larger section area, to produce more lift, and to be less sensitive to leading edge roughness [3]. Therefore, blunting trailing-edge airfoils could further improve both the structural strength and the aerodynamic performance of large wind turbine blades.

However, the comparatively high airfoil thickness simultaneously increases drag penalty, which is mainly caused by flow separation at large angles of attack. Due to increasing angles of attack, adverse stream-wise pressure gradients increase correspondingly and lead to a separation of flow. Airfoil thickness increases from tip to root, as well as the reduction of wind velocity, which is not ideal for low Reynolds number flows [4]. It is particularly problematic for flow separation in the region near the hub [5]. Consequently, the efficiency of wind turbines is diminished by the drag penalty resulting from flow separation [6]. Thus, it is a crucial objective to study the flow separation control methods for better aerodynamic performance of wind turbines.

Vortex generators (VGs), first documented by Taylor [7], are widely-used effective flow separation control devices. In 1990, Afjeh [8] predicted the aerodynamic performance of a horizontal-axis wind turbine equipped with VGs. In 1995, Øye [9] indicated that a stall-regulated wind turbine power increased nearly 24% by using VGs (from 850 kW to 1050 kW) through field tests. The first industrial application was implemented by UpWind Solutions, Inc. [10] in 2012 and the result showed that the mean Annual Energy Production (AEP) increase experienced within the 3 month time period was in the range of 2.1–2.5%. And then, a relation between wind speeds and the impact of VGs on AEP was pointed out. Therefore, VGs are effective devices for wind turbines to increase power output and studies are required for VGs to further improve wind turbine performance.

Many researches have been carried out towards VGs on wind turbines. Lin [11] reviewed the research on low-profile VGs to control boundary separation, and summarized the features of different types of VGs and their applications. He also pointed out that VG is applicable to control flow separation at a relatively fixed point, and its installation location should not far away from the

* Corresponding author. Tel.: +86 10 61772046.
E-mail addresses: linyue816@hotmail.com (L. Gao), yqliu@ncepu.edu.cn (Y. Liu).

http://dx.doi.org/10.1016/j.renene.2014.11.043
0960-1481/

Nomenclature

Latin symbols

a	short spacing between adjacent vortex generators (mm)
b	long spacing between adjacent vortex generators (mm)
c	airfoil chord length (m)
C_d	drag coefficient (dimensionless)
C_l	lift coefficient (dimensionless)
$C_{l,max}$	maximum lift coefficient (dimensionless)
d	length of vortex generator (mm)
ds	the height of first grid layer (m)
h	trailing-edge height of vortex generator (mm)
l	span-wise length (m)
C_l/C_d	lift-to-drag ratio (dimensionless)
Re	Reynolds number (dimensionless)
U_∞	wind speed (m/s)
x, y, z	Cartesian coordinate system
$y+$	dimensionless wall distance

Greek symbols

α	angle of attack (°)
β	angle of incidence of VG vanes (°)
ρ	air density [assumed 1.225 kg/m^3]
μ	dynamic viscosity (Pa s)

Abbreviations

CFD	computational fluid dynamics
VG	vortex generator
DUT	Delft University of Technology

point of separation. The performance of VGs on DU91-W2-250 was experimentally evaluated by Velte et al. [5] using Stereoscopic particle image velocimetry (PIV). Velte and Hansen [12] also investigated the flow behind VGs by Stereoscopic PIV near the stall. Mueller-Vahl et al. [13] investigated the optimization of VG configuration in both experimental and numerical way. Their conclusions were drawn through their observations on force measurements and PIV measurements. Advanced CFD models were established by Xue et al. [14] to capture the micro-scale physics of VGs, and their models were proved to be suitable to uncover the performance of tiny VGs. Yang et al. [15] conducted simulations of aerodynamic performance affected by VGs on blunt trailing-edge airfoils, and they indicated that VGs could also function efficiently on a DU airfoil.

However, the above investigations only focus on blunt trailing-edge airfoils or performance of VGs on sharp trailing-edge airfoils. The present researches on blunt trailing-edge airfoils equipped with VGs are limited and rare, particularly for parametric study. Therefore, it is significant to have parametric investigations of VGs on blunt trailing-edge airfoil for wind turbines.

To solve the above problem, the study on effects of VGs on airfoil DU97-W-300 has been carried out using CFD simulations in this paper. The organization of the rest of paper is as follows. Section 2 describes the geometric considerations for the blunt trailing-edge airfoil and VGs. Section 3 illustrates the CFD simulations. In Section 4, the impact of VGs' sizes, including trailing-edge height, length, and short and long spacing between adjacent VGs, on DU97-W-300 has been discussed. Section 5 presents the final conclusions.

2. Geometric description

2.1. Blunt trailing-edge airfoils

Blunt trailing-edge airfoils (DU series) were developed by DUT for wind turbines using RFOIL, a modified version of XFOIL [16]. A representative and base airfoil DU97-W-300 with a thick trailing edge of about 1.74% chord has been adopted in this paper, and its maximum thickness locates around 30% chord. Airfoil DU97-W-300 is widely suited to 40% span-wise position of a wind turbine blade, and could smoothly transit to the other airfoils. Additionally, its design goal of the maximum lift coefficient $C_{l,max}$ is in the range of 1.5–1.6 at a Reynolds number of 3×10^6 [17,18].

2.2. Vortex generators

Vortex generators are utilized to suppress the flow separation caused by adverse pressure gradients and turbulence [19], increase lift [20,21] and reduce drag [4] through generating discrete streamwise vortices to energize the slower moving boundary layer with the high-momentum fluid in free stream and in the outer part of the boundary layer [22,23].

Optimization of VGs has been investigated by several authors with the consideration of following variables, but not limited to: type, shape, size, patterns (orientation of adjacent VGs) and location. In this paper, size parameters, including height, length, short and long spacing between adjacent vortex generators, are the key research objectives. Other govern variables were determined according to the optimal solutions in Refs. [11,13,17,24].

Fig. 1 portrays two main configurations of VGs, the counter-rotational configuration and the co-rotational configuration. The adjacent VGs in the co-rotational configuration have all equal angles of incidence to the flow, while the adjacent VGs in the counter-rotational configuration possess equal, but opposite angles of incidence. The rotational directions of vortices generated by a pair of VGs depend on their array configurations. The counter-rotational configuration has been proved to be more effective to suppress the flow separation in several aerodynamic applications [24–26]. The same result for wind turbines was obtained by our early study [27].

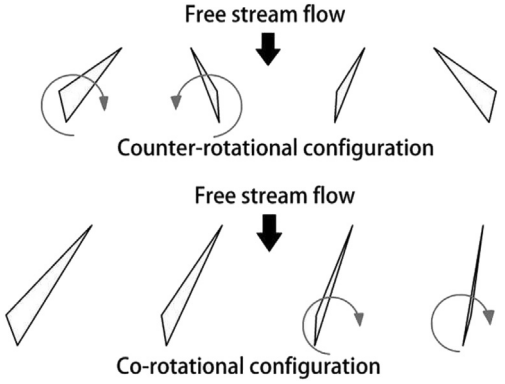

Fig. 1. Schematic of the counter-rotational configuration and the co-rotational configuration.

The chord-wise position of VGs was emphasized and experimentally researched in a recent study by Mueller-Vahl et al. [13], who concluded that the range of $x/c = 15–20\%$ was ideal to realize smooth post-stall lift as well as low drag.

In this paper, VGs are located at 20% chord position in the counter-rotational configuration (see Fig. 3).

3. Simulation methods

3.1. Numerical models

The configuration of VGs with five primary variables in Fig. 2 has been adopted. Table 1 presents the geometric parameters of four delta VGs models. In four cases, VGs1 is the benchmark model, developed and proved to be efficient by DUT. In order to compare with the experimental results [17,18], the models of straight blade sections are of the same size (0.6 m in chord-wise and 0.216 m in span-wise). Five pairs of VGs, which means five cycles, have been arranged to simulate the interaction between the VGs (see Fig. 3).

In all of the four models, the long spacing between adjacent vortex generators *b* is approximately five times of the height of VGs considering the relevant conclusions provided by Mueller-Vahl et al. When the VGs are positioned too close together, a quick decay of vorticity occurs and the flow cannot remain attached to the suction side of the airfoil due to the interaction of the neighboring vortices. On the other hand, spacing the VGs too far apart impairs their ability to suppress flow separation in the intermediate region [13].

The common C–H computational domain has been adopted and the flow domain in the wake is 30 times the chord length. The boundary conditions have been defined as follows. The inlet and outlet have been defined as velocity inlet and pressure outlet, respectively. The airfoil surface, as well as VGs, has been defined as wall. The front and back have been defined as symmetry. The computational domain was meshed with hexahedral structures grids (except for the region between adjacent VGs) and the total number of grid nodes is 2.32 million. The numbers of grid nodes of trailing-edge height *h*, length *d*, short spacing a, long spacing *b* and the hypotenuse of VG are 25, 66, 12, 30 and 33, respectively. Unstructured grids were utilized in the region between adjacent VGs. Fig. 4 shows the geometry of a model with VGs and the local region, where was determined by the analysis of VGs affecting region depicted by Yang et al. [15]. Inside this region, the impact of VGs on flow field is significant, and thus the grids are correspondingly denser than those in external computational domain. In the case of VGs1, the height of first cell layer *ds* is 0.21 mm, indicating $y+$ equals approximately 40. In other cases with VGs, *ds* are of the same value (0.16 mm), indicating $y+$ of the first grid away from the blade surface is about 30, as required for Spalart-Allmaras turbulence model with standard wall function.

The Steady-state computations have been carried out using a commercial CFD solver Fluent. In this study, Reynolds-Averaged Navier–Stokes (RANS) equations have been solved with the Spalart-Allmaras turbulence model, which has been confirmed efficient in Refs. [19,25]. The governing equations used a second-order upwind discretization and solved using the SIMPLE algorithm. Based on the simulation methods, four cases (refer to Table 1), as well as clean model were established and calculated in the range of angles of attack from 0.97° to 20.9° at $Re = 3 \times 10^6$ and $Re = 2 \times 10^6$ (Case VGs1 only).

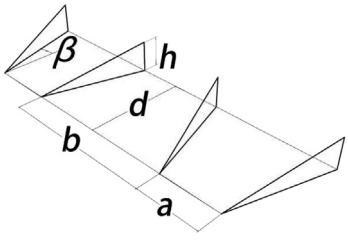

Fig. 2. Geometric parameters of VGs.

Table 1
The main parameters of VGs.

Case no.	*H* [mm]	*d* [mm]	*a* [mm]	*b* [mm]	*β* [°]
VGs1	5	17	10	25	16.4
VGs2	6	17	10	25	16.4
VGs3	6	17	12	30	16.4
VGs4	6	20.4	12	30	16.4

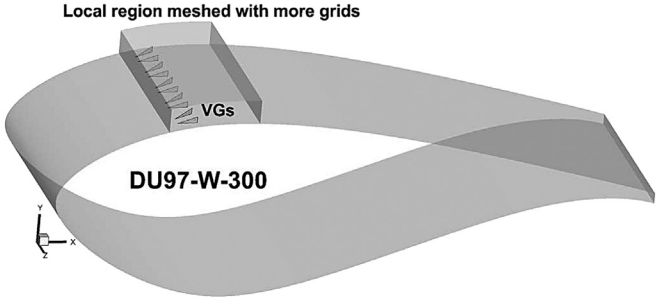

Fig. 3. Geometry of the airfoil DU97-W-300 with VGs.

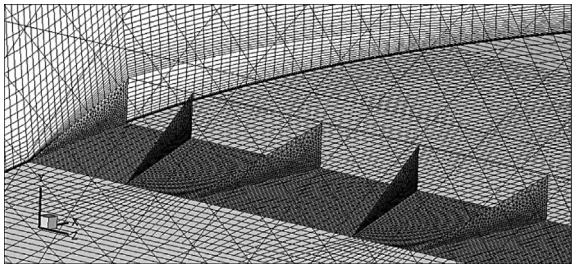

Fig. 4. Mesh in the local region around VGs.

3.2. Validation of the numerical simulations

The simulation results of the clean model and the typical case with VGs (VGs1) have been validated through the comparison with the experimental data [17]. As shown in Fig. 5(a), the CFD results of lift coefficients are well matched with wind tunnel experimental data, and they have an excellent agreement at the stall angle of attack. The drag coefficient curve is consistent with the one plotted using experimental data within a mean relative error limit of 8%. Fig. 5(b) shows that the lift coefficient curves of the simulation coincide well the experimental data. The simulation results of drag coefficients are slightly higher than the experimental results, which might be caused by the limitations of the turbulence model. For numerical simulations, it is difficult to precisely calculate the drag coefficients due to their small values and a mean relative error limit (less than 10%) is acceptable. In these two cases, the stall angle of attack and lift coefficients are well simulated, and the differences from the numerical and experimental results of drag coefficients are acceptable. Therefore, the CFD simulations merit the further study.

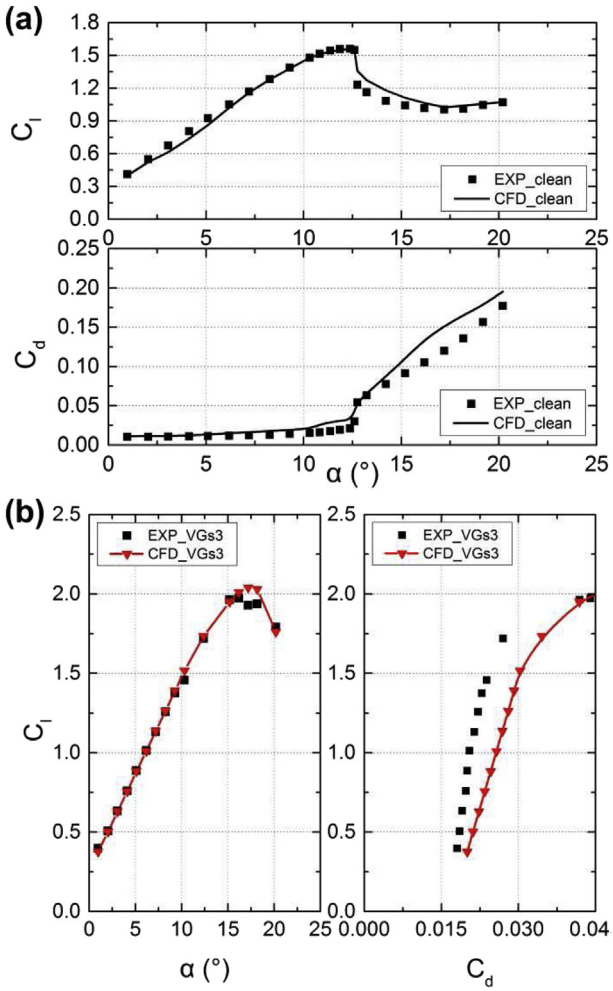

Fig. 5. Comparison between CFD results and experimental data for DU97-W-300. (a) Lift coefficients and drag coefficients of the clean model at $Re = 3 \times 10^6$. (b) Lift coefficients and drag coefficients of VGs1 at $Re = 2 \times 10^6$.

4. Results and discussion

In order to investigate the parametric effects of VGs on the blunt trailing-edge airfoil DU97-W-300, aerodynamic properties, such as stall angles of attack, lift coefficients, drag coefficients and lift-to-drag ratios, have been presented. Additionally, the two-dimensional and three-dimensional streamlines and vortices in the wake region have been analyzed to help further explain the results.

4.1. Effects of VG trailing-edge height on DU97-W-300

As shown in Fig. 6, the impact of VGs on the blunt trailing-edge airfoil performance is presented through the comparison between cases with and without VGs. In Fig. 6(a), it is clear to see that the lift coefficients increase linearly with the angle of attack until flow separation begins to have effects. For cases with VGs (VGs1 and VGs2), the lift coefficient curves are generally consistent with that of the clean model before stall, while there is a slight drag penalty resulting from the induced friction by adopting VGs. As the angle of attack increases, stall phenomenon appears and VGs help the airfoil increase the stall angle of attack compared to the clean model approximately from 12° to 17°. The maximum values of lift coefficient $C_{l,max}$, which occur just prior to the stall, are pronouncedly

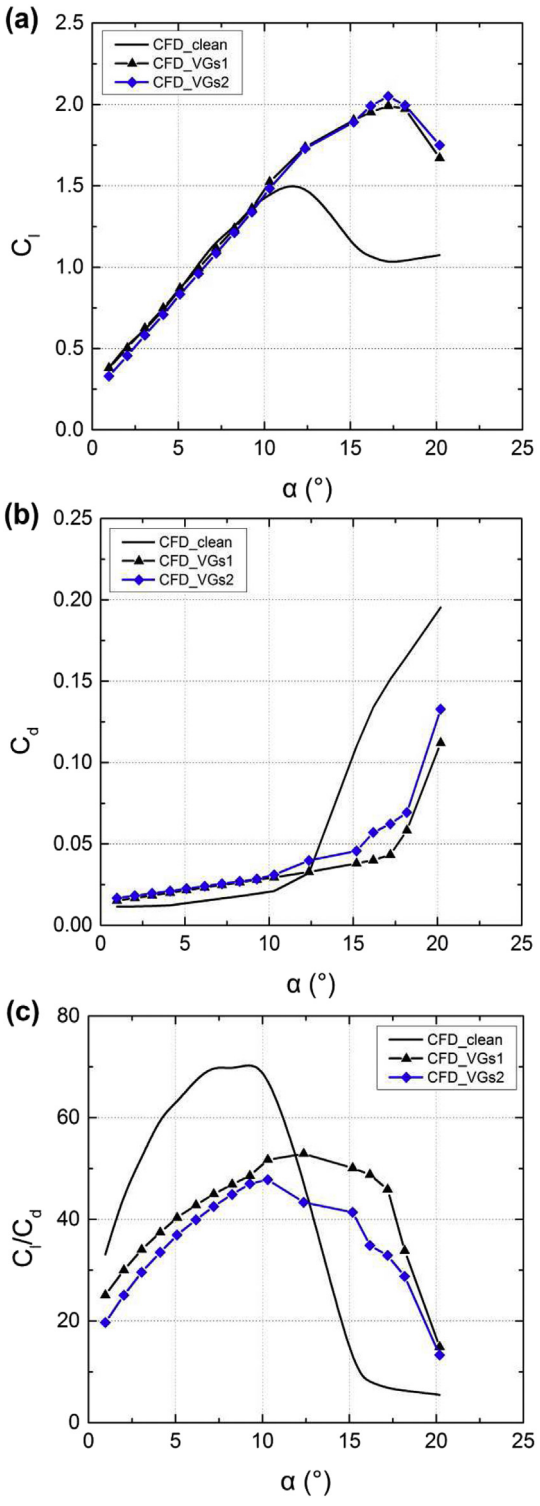

Fig. 6. Impact of VG trailing-edge height on DU97-W-300 at $Re = 3 \times 10^6$. (a) Comparison of lift coefficient curves. (b) Comparison of drag coefficient curves. (c) Comparison of lift-to-drag ratio curves.

increased by using VGs. Beyond the stall angle, a large decrease in lift and a precipitous increase in drag are yielded due to the separated flow and VGs are seen to be beneficial for the reduction of pressure drag caused by flow separation (more description later), as shown in Fig. 6(b). Additionally, the lift-to-drag ratio presented in Fig. 6(c) indicates that the airfoil is positively influenced by VGs at

high angles of attack at an inevitable cost of a decrease in the $(C_l/C_d)_{max}$.

Fig. 6 also shows the effects of VGs' height on airfoil performance. Compared with VGs1, VGs2 possesses a larger trailing-edge height h, and other parameters are of the same values. The comparison of lift coefficient curves is given in Fig. 6(a). The trailing-edge height is evaluated considering both lift increase and drag penalty. A better performance of lift is achieved in the case of VGs2, where a higher value of $C_{l,max}$ is yielded at $\alpha = 17.2°$ compared to VGs1. However, VGs2 produces a larger increase in drag due to the excessive friction caused by the larger height, as shown in Fig. 6(b), which in turn has a negative impact on the lift-to-drag ratio.

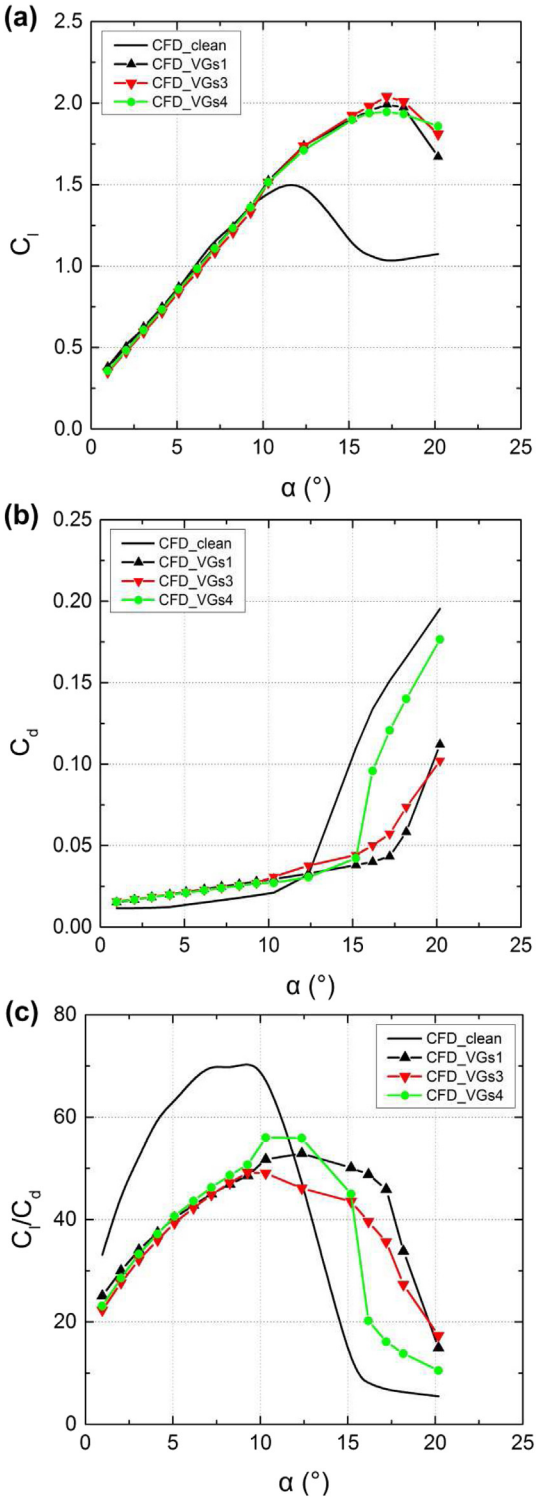

Fig. 7. Impact of VG length on DU97-W-300 at $Re = 3 \times 10^6$. (a) Comparison of lift coefficient curves. (b) Comparison of drag coefficient curves. (c) Comparison of lift-to-drag ratio curves.

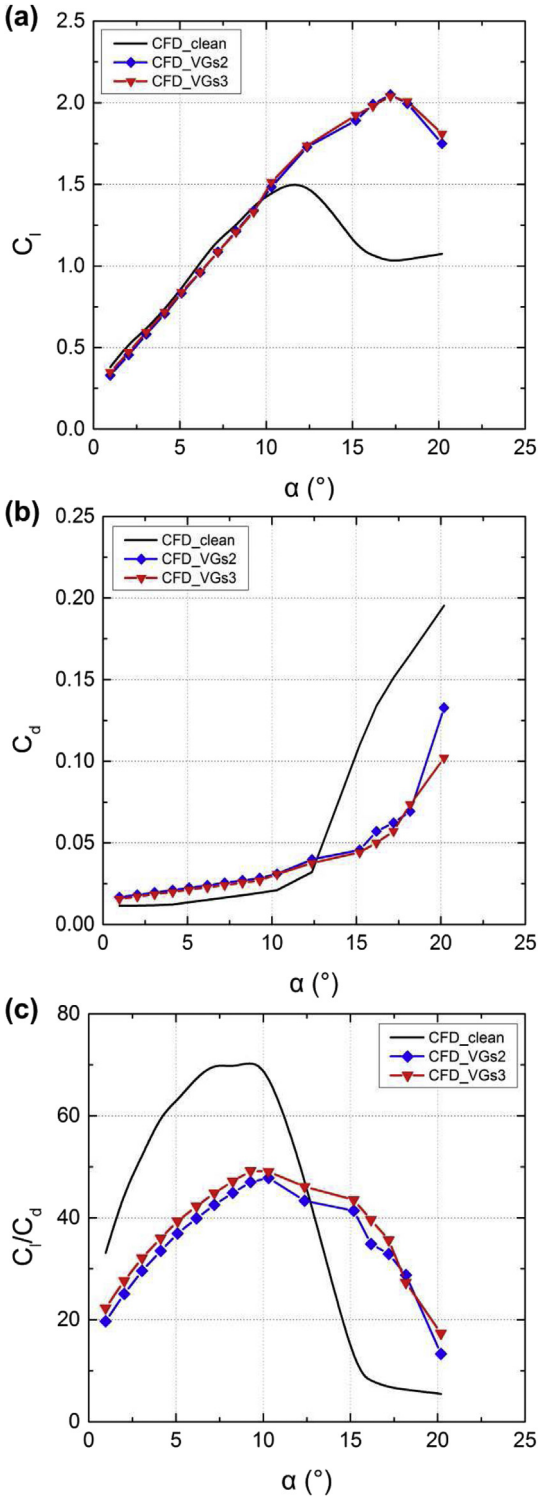

Fig. 8. Impact of short and long spacing between adjacent VGs on DU97-W-300 at $Re = 3 \times 10^6$. (a) Comparison of lift coefficient curves. (b) Comparison of drag coefficient curves. (c) Comparison of lift-to-drag ratio curves.

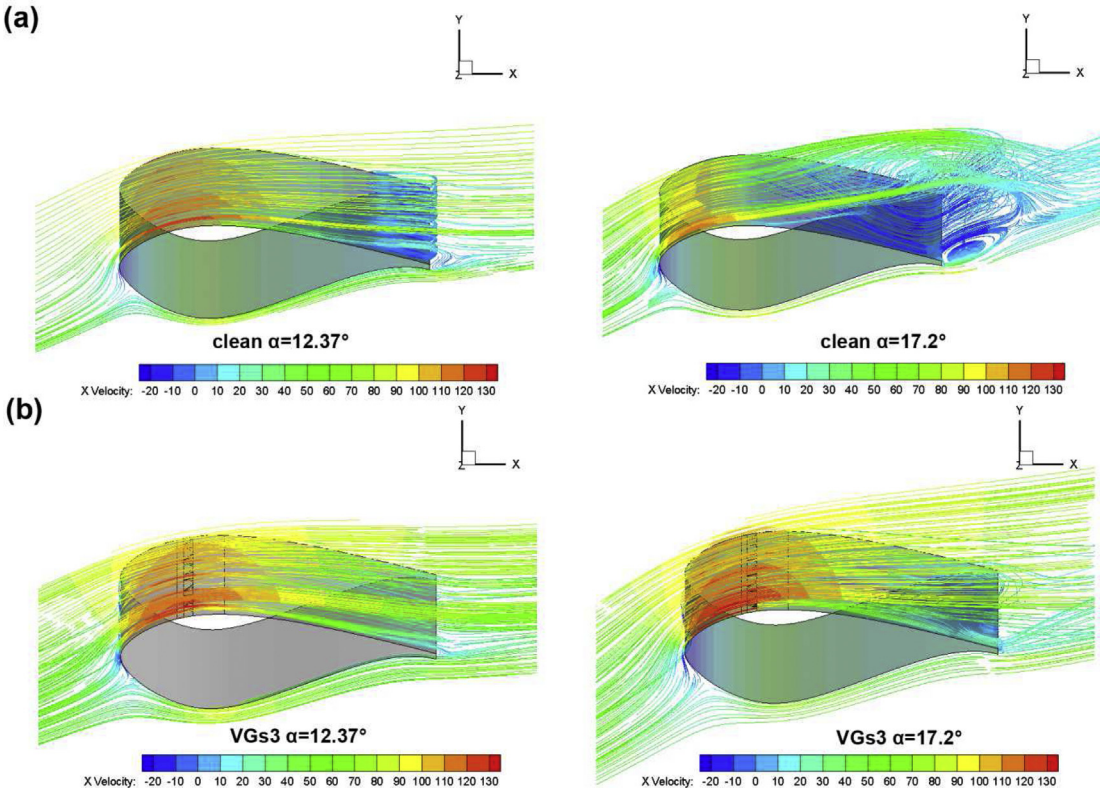

Fig. 9. Comparison of three-dimensional streamlines among models with and without VGs. (a) Three-dimensional streamlines of the clean model at $\alpha = 12.37^{\circ}$ and $\alpha = 17.2^{\circ}$. (b) Three-dimensional streamlines in the case of VGs3 at $\alpha = 12.37^{\circ}$ and $\alpha = 17.2^{\circ}$.

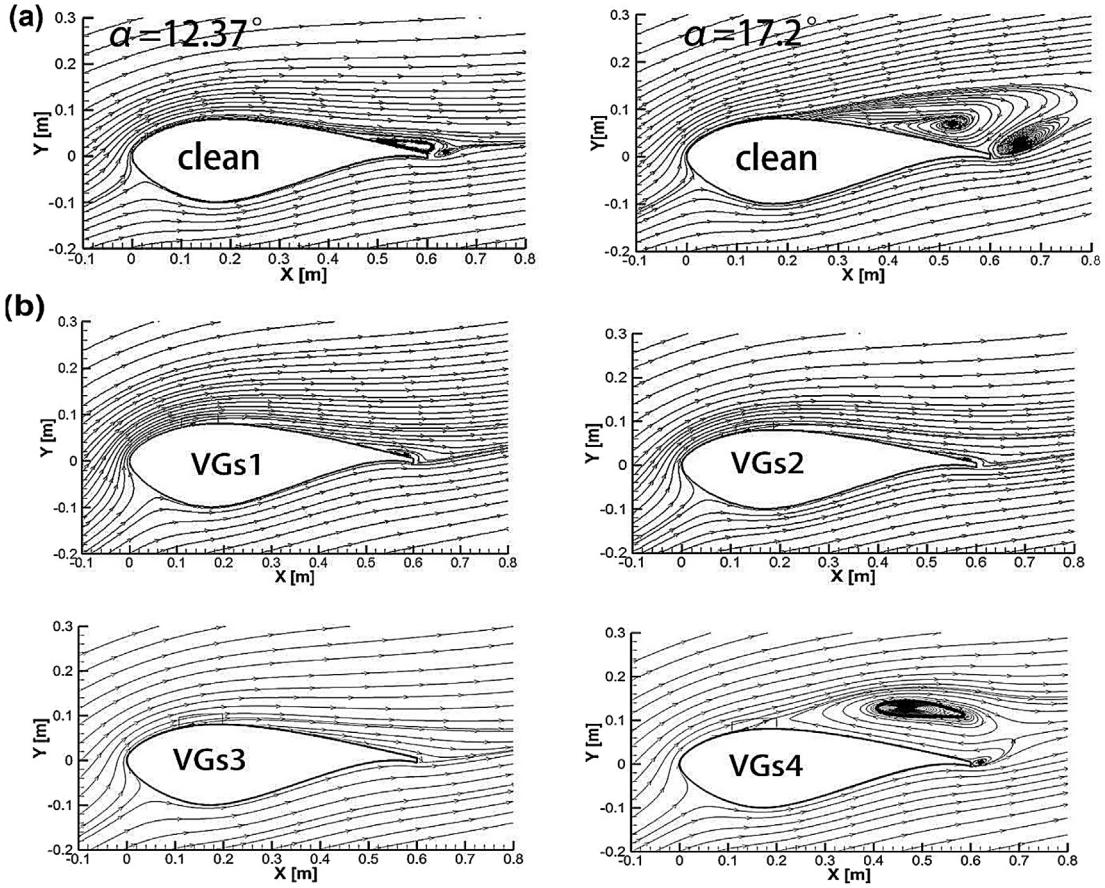

Fig. 10. Comparison of two-dimensional streamlines among models with and without VGs. (a) Two-dimensional streamlines of the clean model at $\alpha = 12.37^{\circ}$ and $\alpha = 17.2^{\circ}$. (b) Two-dimensional streamlines in the cases with VGs at $\alpha = 17.2^{\circ}$.

4.2. Effects of VG length on DU97-W-300

The impact of the different length of VGs on the airfoil is given in Fig. 7. VGs3 and VGs4 are two models with the same size, except for length. The length of VGs4 (20.4 mm) is larger than that of VGs3 (18 mm). At angles beyond static stall angle, VGs3 performs better to ameliorate the lift coefficients and the maximum lift coefficient. Meanwhile, the drag of VGs4 increases compared to VGs3, indicating that drag increases corresponding to extension of length.

Fig. 7 also shows a comparison between VGs1 and VGs4 with respect to lift and drag. VGs4 is 6/5 times as large as VGs1 in all dimensions, sharing a similar geometry. VGs1 present a much better performance in lift increase and drag decrease at high angles of attack. Although VGs4 produces stronger vortices for its larger dimensions (see Fig. 11), it doesn't mean that it owns a better flow separation control performance. When the angle of attack is around 15°, a sharp, precipitous increase in drag coefficients occurs in the case of VGs4 resulting from its failure to suppress the separated flow (refer to the streamlines in Fig. 10). Generally, VGs1 is superior to VGs4 in aerodynamic performance improvement of airfoil DU97-W-300 in addition to the maximum lift-to-drag ratio.

4.3. Effects of spacing between adjacent VGs on DU97-W-300

The impact of short and long spacing between an adjacent pair of VGs on DU97-W-300 is given in Fig. 8. The ratio between the short spacing a and the long spacing b is two to five. The spacing

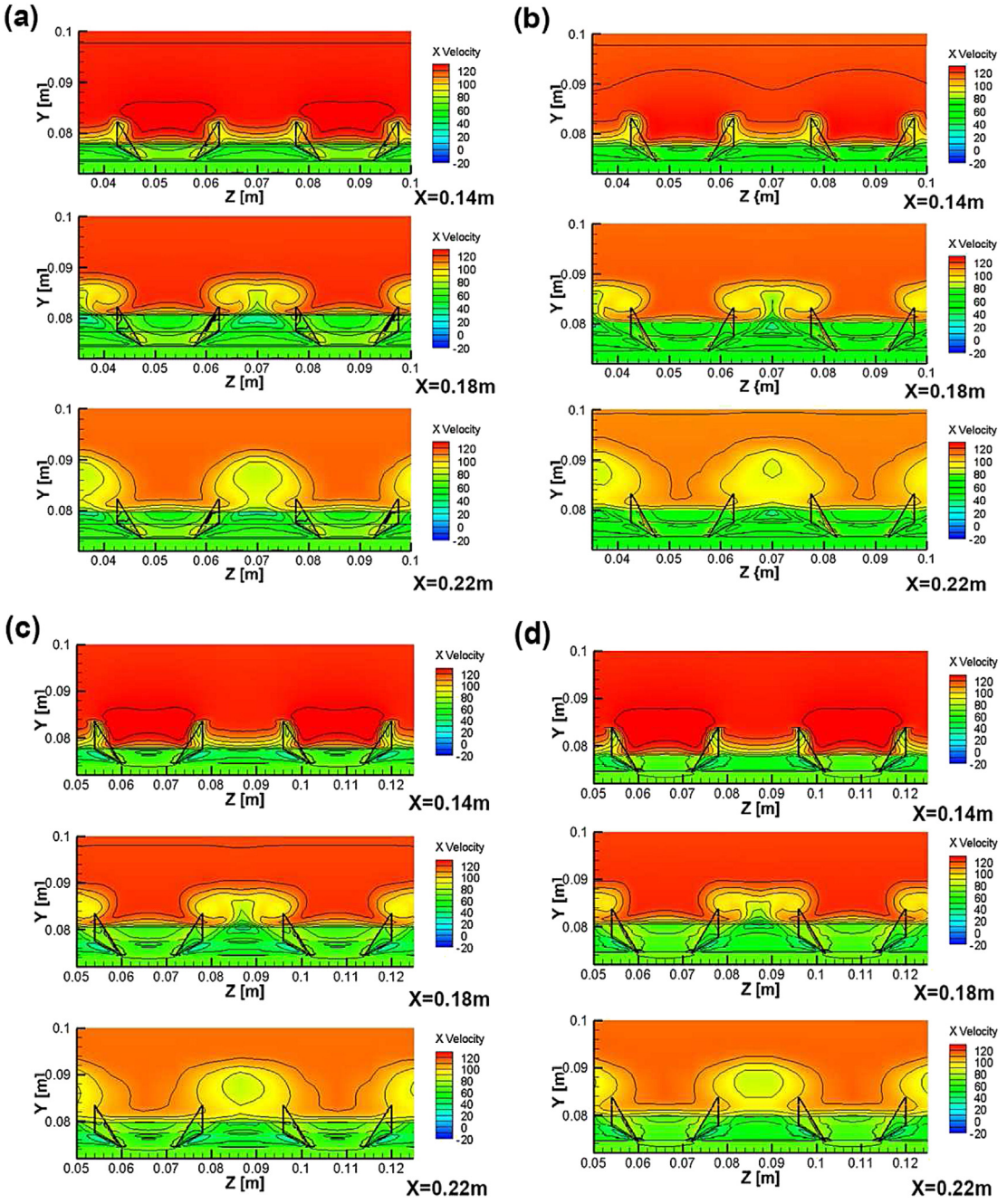

Fig. 11. *X*-velocity contours in the downstream region of VGs, at $\alpha = 10.31°$.

parameters a and b in the case VGs3 are 6/5 times the VGs2's, respectively.

As shown in Fig. 8(a), the lift coefficients of VGs2 and VGs3 are mainly consistent with each other at all the angles of attack beyond stall in addition to $\alpha = 21°$. The drag coefficients of VGs2 are slightly larger than VGs3's in the range of about 12°–18° angles of attack (see Fig. 8(b)). C_d of VGs2 surges at $\alpha = 21°$, which is mainly a result of the abrupt flow separation on the suction side of the airfoil. In the case of VGs3, a relatively smooth transition in drag is presented due to the larger spacing. The $(C_l/C_d)_{max}$ in the case of VGs3 is higher than that of VGs2 for the decrease in drag, as can be seen in Fig. 8(c).

4.4. Analysis of flow field around VGs

In order to further explain the aerodynamic performance of VGs on the blunt trailing-edge airfoil, the flow field around VGs has been analyzed. Fig. 9 shows the comparison of three-dimensional streamlines between models with and without VGs at typical angles of attack. In Fig. 9(a), at a relatively low angle of attack $\alpha = 12.37°$, the flow moves smoothly over the suction side of the airfoil. As angle of attack increases, flow for the clean model cannot remain attached to the suction side of surface and it tends to gradually separate from the trailing edge toward the leading edge. Inside the separated region (in dark blue, in the web version), it is clear to see the reversed flow which is in an opposite direction to the free stream. Compared to the clean model, there is no obvious flow separation in the case of VGs3 at the same angles of attacks, as shown in Fig. 9(b).

Additionally, compared with the clean case, flow can be attached well to the surface at $\alpha = 17.2°$ in the cases with VGs, except the case of VGs4, as can been seen in Fig. 10. In the case of VGs4, vortices are easily observed and the velocity in the wake of VGs decreases quickly. The capability of momentum exchange between boundary layer and free stream is diminished, and consequently the ability to control flow separation is limited in this case in contrast with other models with VGs. The overall larger dimensional parameters are thus not responsible for a better flow separation control performance.

The X-velocity contours in the wake region of VGs when $\alpha = 10.31°$ are presented for four cases, as shown in Fig. 11. Three span-wise positions $X = 0.14$ m, $X = 0.18$ m and $X = 0.22$ m (corresponding to 23% chord, 30% chord and 37% chord, respectively) were selected. As X increases, counter-rotating vortices gradually expand in the downstream region. Flow in the intermediate region between a converging pair of VGs (upwash region) is in a lower velocity than that between a diverging pair of VGs (downwash region). The flow in opposite directions generates two counter-rotating vortices between a converging pair of VGs, as can be seen at $X = 0.18$ m in Fig. 11. In this way, the induced vortices help energize the slower moving flow near the surface with high-momentum air in free stream. The comparison among the four cases shows that the VGs with relatively larger trailing-edge height generate stronger vortices. Appropriately enlarging the spacing between an adjacent pair of VGs has positive influence on keeping the vortices attached to the suction side of the airfoil and expanding the span-wise region affected by vortices.

5. Conclusions

In this paper, the three-dimensional models with and without VGs were established and validated to be capable of analyzing the parametric effects of VGs on the blunt trailing-edge airfoil DU97-W-300. The main conclusions were:

1) VGs are effective to produce a significant increase in both the maximum lift coefficient and the static stall angle of attack for the blunt trailing-edge airfoil. The drag pronouncedly decreases beyond stall by using VGs at a cost of a slight drag penalty before stall.
2) An increment of VG trailing-edge height is beneficial for VG to generate vortices with higher momentum, which brings an increase in lift as well as the maximum lift coefficient of the airfoil DU97-W-300. However, a drag penalty is also yielded, which leads to a reduction of lift-to-drag ratio.
3) Extending of VG length leads to negative influence on both lift and drag.
4) An appropriate enlargement of both long and short spacing between an adjacent pair of VGs contributes to keeping the vortices attached to the suction side of the airfoil and expanding the downstream area affected by vortices in span-wise, which has positive influence on flow separation control.
5) VGs in larger dimensions generate stronger vortices, which doesn't necessarily lead to a better control of flow separation.

The further study will focus on the combined impact of two VGs' parameters on blunt trailing-edge airfoils.

Acknowledgments

The authors are grateful to National Natural Science Foundation of China (Grant No. 51376062, No. 51306055). Also many thanks to WANG X.D. from Key Laboratory of Condition Monitoring and Control for Power Plant Equipment, Ministry of Education, North China Electric Power University for the fruitful discussions.

References

[1] Fischer GR, Kipouros T, Savill AM. Multi-objective optimisation of horizontal axis wind turbine structure and energy production using aerofoil and blade properties as design variables. Renew Energy 2014;62:506–15.
[2] Lago LI, Ponta FL, Otero AD. Analysis of alternative adaptive geometrical configurations for the NREL-5 MW wind turbine blade. Renew Energy 2013;59:13–22.
[3] Berry D, Lockard S. Innovative design approaches for large wind turbine blades final report. SAND2004-0074. Albuquerque, NM: Sandia National Laboratories; 2004.
[4] Nicherson JD. A study of vortex generators at low Reynolds numbers. AIAA paper. 1986.
[5] Velte CM, Hansen MOL, Meyer KE, Fuglsang P. Evaluation of the performance of vortex generators on the DU 91-W2-250 profile using stereoscopic PIV. J Syst Cybern Inform 2009;7:92–6.
[6] Chamorro LP, Arndt REA, Sotiropoulos F. Drag reduction of large wind turbine blades through riblets: evaluation of riblet geometry and application strategies. Renew Energy 2013;50:1095.
[7] Taylor HD. The elimination of diffuser separation by vortex generators. Report no. R-4012-3. United Aircraft Corporation Connecticut, Research Department; 1947.
[8] Afjeh AA, Keith TG, Fateh A. Predicted aerodynamic performance of a horizontal-axis wind turbine equipped with vortex generators. J Wind Eng Ind Aerodyn 1990;33:515–29.
[9] Øye S. The effect of vortex generators on the performance of the ELKRAFT 1000 kW turbine. 1995.
[10] UpWind solution case study on impact of vortex generators on wind turbine performance. UpWind Solutions, Inc; 2013.
[11] Lin JC. Review of research on low-profile vortex generators to control boundary-layer separation. Prog Aerosp Sci 2002;38:389–420.
[12] Velte CM, Hansen MOL. Investigation of flow behind vortex generators by stereo particle image velocimetry on a thick airfoil near stall. Wind Energy 2013;16(5):775–85.
[13] Mueller-Vahl H, Pechlivanoglou G, Nayeri CN, Paschereit CO. Vortex generators for wind turbine blades: a combined wind tunnel and wind turbine parametric study. Am Soc Mech Eng 2012:899–914.
[14] Xue S, Johnson B, Chao D, Sareen A, Westergaard C. Advanced aerodynamic modeling of vortex generators for wind turbine applications. 2010.
[15] Yang K, Zhang L, Xu J. Simulation of aerodynamic performance affected by vortex generators on blunt trailing-edge airfoils. Sci China Ser E Technol Sci 2010;53:1–7.
[16] Drela M. XFOIL: an analysis and design system for low Reynolds number airfoils. Low Reynolds number aerodynamics. Springer; 1989. p. 1–12.

[17] Timmer WA, Van Rooij RPJOM. Summary of the Delft University wind turbine dedicated airfoils. J Sol Energy Eng 2003:488–96.
[18] Timmer WA, Schaffarczyk AP. The effect of roughness at high Reynolds numbers on the performance of aerofoil DU 97-W-300Mod. Wind Energy 2004;4:295–307.
[19] Schubauer GB, Spangenberg WG. Forced mixing in boundary layers. J Fluid Mech 1960;01:10–32.
[20] Bragg MB, Gregorek GM. Experimental study of airfoil performance with vortex generators. J Aircr 1987;24:305–9.
[21] Storms BL, Jang CS. Lift enhancement of an airfoil using a Gurney flap and vortex generators. J Aircr 1994;31:542–7.
[22] Lin JC, Robinson SK, McGhee RJ, Valarezo WO. Separation control on high-lift airfoils via micro-vortex generators. J Aircr 1994;31:1317–23.
[23] Wendt BJ, Hingst. Flow structure in the wake of a wishbone vortex generator. AIAA J 1994;32:2235.
[24] Bray TP. A parametric study of vane and air-jet vortex generators. 1998.
[25] Godard G, Stanislas M. Control of a decelerating boundary layer. Part 1: optimization of passive vortex generators. Aerosp Sci Technol 2006;10:181–91.
[26] Jirasek A. Vortex-generator model and its application to flow control. J Aircr 2005;42:1486–91.
[27] Dai L, Zhang H, Jiao J, Li X, Kang S. Characterization of vortex generators induced flow around wind turbine airfoil. Appl Mech Mater 2013;448–453:1779–84.